Cement and Concrete Composites 73 (2016) 1–9

Contents lists available at ScienceDirect

Cement and Concrete Composites

journal homepage: www.elsevier.com/locate/cemconcomp

Monitoring and modelling the early age and hardening behaviour of eco-concrete through continuous non-destructive measurements: Part II. Mechanical behaviour

Jérôme Carette*, Stéphanie Staquet

Université Libre de Bruxelles (ULB), Service BATir, Belgium

ARTICLE INFO

Article history:
Received 24 January 2016
Received in revised form
21 June 2016
Accepted 4 July 2016
Available online 7 July 2016

Keywords:
Ultrasonic pulse velocity
Hydration degree
Early age
Mechanical properties
Elastic modulus

ABSTRACT

A recent scientific and industrial interest has been brought to combine multiple supplementary cementitious materials (SCM) in large quantities in concrete binders. The growing use of binary, ternary or quaternary cement binders calls for the development of simple, efficient and accurate experimental and numerical means to characterise and predict the behaviour of such concretes. Continuous non-destructive testing constitutes a major opportunity since it generally consists in simple test setup requiring low human interaction. In this study, isothermal calorimetry and ultrasonic pulse velocity (compression and shear waves) are performed on various concrete compositions with massive incorporation of limestone filler and blast-furnace slag. Indeed, these two additions present interesting complementary effects and positive synergies in terms of fresh properties, mechanical behaviour and durability potential. The setting time, compressive and tensile strength and elastic modulus of these concretes is investigated from the setting time to the hardened state. The existing models linking these properties to the hydration degree, ultrasonic pulse velocity or hydration time are not applicable to these materials, especially during the early age period. New models are proposed and validated for the early age behaviour of concrete with SCMbased binders.

1. Introduction

In the first part of this study [1], continuous non-destructive testing (CNDT) such as isothermal calorimetry (IC) and ultrasonic pulse velocity (UPV) were used to monitor the heat flow, degree of hydration and apparent activation energies of various concrete compositions containing various amounts of limestone filler (LMF) and blast furnace slag (BFS). Indeed, LMF and BFS present interesting complementary effects and positive synergies in terms of fresh properties, mechanical behaviour and durability potential [2–10].

As regards the mechanical properties of these materials, the degree of hydration can be correlated to the setting time [11–13], strength evolution [14,15], or elastic properties [14–16]. Complementarily, UPV measurements can be correlated to the mechanical properties of concrete such as setting time [17–20], strength [21–24] and elastic properties [16,25,26]. These correlations are generally obtained through the measurement of compression waves (P-waves), and are mostly dependent on the water/cement ratio, nature and amount of the binder. In addition, these correlations are not satisfactory to represent the early age behaviour of concrete, as it will be discussed in this paper.

In this second part, the compressive strength, tensile splitting strength, and elastic modulus of five concrete compositions are investigated through classical measurements and correlated with various CNDT methods. This paper aims at:

- improving continuous non-destructive alternatives to the measurement of some of the main concrete mechanical properties
- assessing and improving the current time-based, degree of hydration-based and UPV-based models of these concrete properties,
- adapting these models to the very early age, hardening and hardened behaviour of concrete,
- ensuring an applicability of these models to all tested concretes compositions, containing high amounts of LMF and/or BFS and variable w/c ratio.

* Corresponding author.
E-mail address: jecarett@ulb.ac.be (J. Carette).

http://dx.doi.org/10.1016/j.cemconcomp.2016.07.003
0958-9465/

2. Materials and method

2.1. Mix designs

The physical and chemical properties of the used materials (aggregates, cement, limestone filler, blast-furnace slag, gypsum) are described in the first part of this study and in other publications [1,20]. In this second part, five concrete compositions are studied (Table 1). The compositions C1, C2, C3 and C4 are identical to the ones tested in the first part, containing respectively PC, PC + BFS, PC + LMF, and PC + BFS + LMF. Then, a fifth composition (C5) is investigated. It contains higher water content (with PC/water ratio identical to C3), reaching a water/binder ratio of 0.57. This is done in order to correspond to the water/reactive ratio (w/r) of compositions containing limestone filler, which is not a reactive compound. For instance, concrete C3 contains 30% of LMF. Therefore, its water/binder ratio is 0.4, while its water/reactive ratio is 0.57. All compositions present the same granular skeleton, water content, paste volume and sulphate content. As explained and justified in Refs. [1], no superplasticizers were used even though low slumps are observed for C1 and C2.

2.2. Test setups

2.2.1. Ultrasonic pulse velocity

The P-wave and S-wave velocity (V_P and V_S respectively) were measured with a device presented in Refs. [20], thus allowing a computation of the dynamic elastic properties with Eqs. (1) and (2), with ρ the density of concrete, ν_d the dynamic Poisson's ratio and E_d the dynamic Young's modulus.

$$\nu_d = \frac{1 - 2\left(V_S^2 / V_P^2\right)}{1 - 2\left(V_S^2 / V_P^2\right)} \tag{1}$$

$$E_d = 2\, V_S^2 \rho\, (1 + \nu_d) \tag{2}$$

2.2.2. Isothermal calorimetry

The heat of hydration of mortars was measured with a TAM AIR isothermal heat conduction calorimeter. The heat release (Q(t)) is measured by comparison between an active (sample) and an inert (sand) cell, both equipped with heat flow sensors. In the first part of this study [1], a methodology is developed to determine the degree of hydration from such measurements, by using a modified version of the model first developed by Freisleben-Hansen and Pedersen (FHP model). This modified model is shown in Eqs. (3)–(5).

$$Q(t) = a_1 \cdot e^{-\frac{\tau_1}{t}^{\beta_1}} + a_2 \cdot e^{-\frac{\tau_2}{t}^{\beta_2}} \tag{3}$$

$$Q_\infty = a_1 + a_2 \tag{4}$$

$$\alpha(t) = \frac{Q(t)}{Q_\infty} \tag{5}$$

Table 1
Composition and properties of concrete mixtures (kg/m^3).

	C1	C2	C3	C4	C5
Aggregate 10/14	873	873	873	873	873
Aggregate 6/10	210	210	210	210	210
Sand 0/4	853	853	853	853	853
Cem I 52.5	432	104	285	103	349
GGBFS	0	291	0	164	0
LMF	0	0	126	124	0
Gypsum	0	22	10	22	0
Water	173	167	169	165	199
Density [kg/m^3]	2540	2519	2525	2514	2484
w/b	0.4	0.4	0.4	0.4	0.57
w/r	0.4	0.4	0.57	0.57	0.57
E_a [kJ/mol]	35.9	49.7	39.1	52	35.9
E_s 28d	51.8	51.7	48.4	50.0	45.0
f_c 28d	53.2	38.7	46.4	33.8	32.2
f_c 90d	58.3	44.0	48.6	39.6	38.3
f_c 365d	61.4	49.6	52.3	46.3	43.1
slump class	S1	S1	S3	S2	S3

2.2.3. Compressive and tensile strength

The compressive strength is measured on 100 × 100 × 100 mm concrete samples. An equivalent strength on cylinder f_c was computed from results on cube $f_{c,cub}$ with Eq. (6). The tensile strength is computed from the splitting tensile strength ($f_{t,sp}$), as recommended by CEB-FIP MC 90 model [27]. In Eq. 7, F represents the peak load, D the sample diameter, and L the length of the sample.

$$f_c = 0.8 f_{c,cub} \tag{6}$$

$$f_t = 0.9 f_{t,sp} = 0.9 \frac{2 \cdot F}{\pi \cdot D \cdot L} \tag{7}$$

2.2.4. Static elastic modulus

An extensometer for testing of concrete cylinders in compression is used. The design of the extensometer was optimized for very early age measurement of the Young's modulus [28]. It consists in two aluminium rings attached to the concrete by specific anchorage. These anchorages allow transversal displacements due to the presence of adjustable elastic plates. This ensures that no transversal confinement of the sample occurs. Three longitudinal sensors (120° spacing) measure the displacements between the two rings. The will to measure very early age static elastic modulus (E_s) requires taking into consideration various parameters.

First, a surfacing of the sample by placing a fast-setting mortar was preferred to mechanical surfacing due to the really low strength of the sample. This allows unmoulding and surfacing right after the setting. The whole preparation procedure includes surfacing both sides of the cylinder, placing an aluminium foil around the sample in order to avoid desiccation and placing the extensometer. The first measurements can theoretically be performed two hours after final setting. However, at that age, the compressive strength of the sample is still low, especially in presence of BFS. Measurements were not performed prior obtaining a compressive strength of 5 MPa.

For practical reasons, the choice is made to perform tests with a 10 s loading duration up to 1/3 of the concrete strength. This protocol results in loading strain rates varying from 5 to 20μ/s, depending on the concrete age. This low variation in strain rate is not expected to affect significantly the results compared to the reproducibility errors of the measurement [26]. For instance, the increase in the measurement of E_s resulting from this range of strain rates approaches 1% [29], whereas reproducibility errors of up to 10% have been observed.

In order to get around the difficulty related to the very early age measurement of E_s, another test setup is used, called TSTM (Temperature Stress Testing Machine). Its mould consists in a horizontal dog-bone shaped formwork surrounded by a thermal regulation.

One of the two heads of the sample is linked to a 400 kN electro-mechanical jack. One of the many potential uses of this equipment consists in performing loadings from as soon as setting has occurred, and therefore provides a corresponding value of E_s. Loadings can then be repeated at a chosen rate in order to obtain the evolution of E_s. Displacements are measured by contact-free electromagnetic sensors at two anchorage points spaced from 750 mm (Fig. 1). The general methodology and device used for these tests was previously thoroughly described [30]. Part of the results were also presented elsewhere [20].

The NDT feature of the latter is debatable. Even if such stress levels are generally considered as non-destructive, secondary early age effects such as load-induced hydration or micro-cracks at the paste-aggregate interface can hardly be confirmed or inferred. In any case, similar values can be obtained when several loadings are applied on one sample in comparison with standard testing, which tends to indicate that such phenomenon are not significant [26]. It remains that the amplitude and number of loading cycles of such tests was limited to a minimum.

The chosen testing protocol is as follows. Loads are applied on the sample at time intervals varying from 30 min to 3 h at 10% of its actual compressive strength. This low value is adopted as to ensure that a loading has no impact on the further properties of the sample. The loadings are applied in 10 s. As for the extensometer, the strain rate is slightly variable between one cycle and another cycle ranging from 1 to 10 μ/s.

3. Results and discussion

3.1. Setting time

The initial and final setting times are defined based on the ultrasonic measurements according to [19]. The initial setting occurs when V_S reaches its maximum rate of increase, and the final setting is reached when E_d increases with its maximum rate. The initial and final setting times summarized in Table 2 were already presented elsewhere [20]. The degree of hydration corresponding to these times are indicated in the same table according to the Q-FHP model.

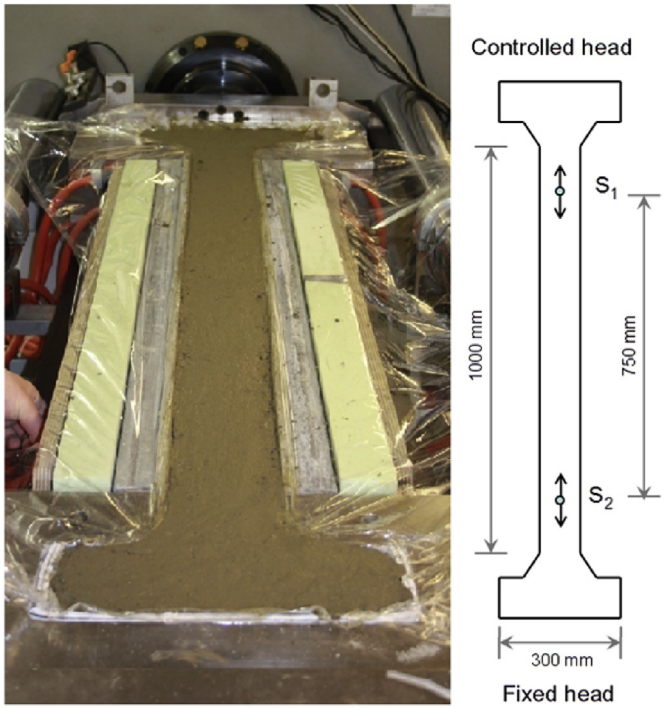

Fig. 1. Design of the used TSTM device.

Table 2
Initial and final setting times and the corresponding hydration degrees.

	t_i [h]	t_f [ ]	α_{ti} [−]	α_{tf} [−]
C1	3.5	4.1	0.013	0.020
C2	6.1	8.5	0.019	0.043
C3	3.9	4.6	0.022	0.034
C4	4.6	6.7	0.022	0.049
C5	5.1	5.9	0.025	0.034

The final setting occurs at a degree of hydration of less than 0.05 for all compositions. This value is significantly lower than generally accepted values of α_0. This point will be discussed further. It is observed that both the water content and the binder nature modifies the hydration degree at which the initial and final setting occur (α_{ti} and α_{tf} respectively), which is a well-known fact, as reviewed and confirmed in Ref. [19]. As expected, increased w/c (C5 versus C1) increases both α_{ti} and α_{ti}. This is due to an increased inter-particle spacing, and therefore to a need for more hydration products formation to form continuous solid paths. On the other hand, both the LMF and BFS increase α_{ti} and α_{tf}. In the case of the former, since LMF is mainly inert [20], this is due to an increased amount of water available for the hydration of PC. As a matter of fact, C5 and C3 present similar α_{ti} and α_{tf} for a similar water/reactive content. In the case of BFS, it might induce further increase of α_{tf} since its main hydration peak has not occurred yet. The composition C4 shows a combination of the above observations, leading to the highest α_{tf}.

3.2. Compressive and tensile strength

The compressive strength for all composition is presented in Fig. 2a. All points correspond to an average of at least three samples performed on at least two batches of concrete. C5 is characterised by a slower increase in the compressive strength in comparison with C1. Its ultimate value is the lowest between all compositions. On the other hand, C3 also shows a slight delay in the increase of compressive strength due to the dilution effect of LMF, but exhibits significantly higher compressive strength for a lower PC content than C5. This confirms the benefit of using LMF, even in high content close to 30%. As regards the concrete containing slag (C2 and C4), both are characterised by a very similar compressive strength. This is due to a combination of at least three mechanisms. Firstly, due to the accelerated setting of C4 compared to C2, the former presents higher compressive strength up to approximately 1 day. During the next day of hydration, the main hydration products are formed from the hydration of PC. Since both compositions present the same amount of PC, they present similar f_c development. Secondly, after 2d, the slag hydration results in the further increase of strength. The slag hydration peak occurs slightly sooner for C2 than for C4, counterbalancing the previous effect. Ultimately, the close f_c values between both compositions confirm that a significant part of slag in C2 is not reactive up to at least 365 d.

Similar trends are observed for the tensile strength development in Fig. 2b. However, the effect of increased water content is less important than observed for f_c. The delayed f_t development of C5 is not significant. In fact, contrary to their compressive strength, C2 and C5 exhibit almost identical trends, both in term of final tensile strength and kinetics of development. This clearly indicates that the compressive and tensile strength are not conferred by the same chemo-mechanical mechanisms. While a high w/c ratio can strongly affect the compressive strength, its effect on f_t is mainly a dilution effect due to the lower PC content. A reduction of 20% in

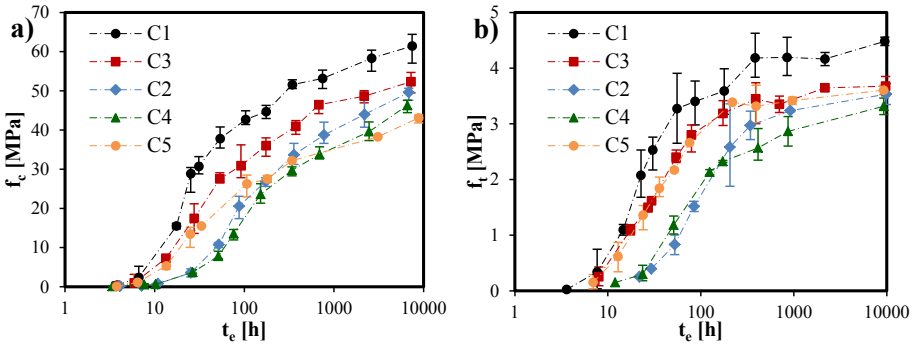

Fig. 2. Evolution of (a) compressive strength and (b) tensile strength as a function of equivalent time from setting time up to 1 year.

the PC content from C1 to C5 induces a 20% decrease in f_t, whatever the concrete age. On the other hand, the lower PC content in C3 indicates that limestone filler also contributes to tensile strength. The similar values of C3 and C5 are the result of the competition between the dilution effect and the inactive or active contribution of limestone filler. The presence of slag has a similar effect on f_c and f_t, including a delay in its development and a slight decrease in the long term strength value.

Three modelling strategies are confronted to the experimental results: a degree of hydration-based model, an equivalent time-based model and a dynamic elastic modulus-based model. They are respectively called hydration model, time model and UPV model.

3.2.1. Hydration model

It is generally considered that before a mechanical percolation threshold, concrete has no mechanical properties. This percolation threshold, which differs from the solid percolation threshold, occurs at a given degree of hydration α_0 [14] close to the final setting time. The evolution of compressive strength, tensile strength or elastic modulus (property X) can be expressed as a function of α_0, $\alpha(t)$, a material parameter a_x (which is property-dependent), and the final value of that property, X_∞ as shown in Eq. (8).

$$X(\alpha) = X_\infty \left(\frac{\alpha(t) - \alpha_0}{\alpha_\infty - \alpha_0} \right)^{a_x} \tag{8}$$

$$X(\alpha) = X_\infty \cdot \alpha(t)^{a_x} \tag{9}$$

However, for the very early age behaviour (around the setting time), it can be observed that the mechanical properties have already developed measurable values. Indeed, in this paper (Table 2) as well as observed in recent studies, the value of α_0 is close to 0.02 [31], or 0.05 [16], which is far from the values originally measured and listed in Ref. [14] between 0.1 and 0.4, probably due to a lack of very early age experimental measurements. Very early age measurements of the compressive strength indicate that at the time of final set, f_c yields around 0.5 MPa [20]. The measurements displayed in Fig. 3 indicate that after the dormant period, any formation of hydration products results in an increase in the mechanical properties, resulting in values of α_0 close to a degree of hydration of 0, whatever the composition.

Considering that $\alpha_\infty = 1$ and that $\alpha_0 = 0$, Eq. (8) becomes Eq. (9). X_∞ and a_x are both obtained by fitting of the model on actual data. Their values as well as the root mean square error (RMSE) are shown in Table 4. The kinetic parameter a_x has no definite value. In other words, its value can hardly be predicted, since it is possibly sensitive to the amount and nature of any SCM or w/b ratio. It is commonly accepted that it has a value close to 1 in compression – this sometime leads to approximate the degree of hydration as a linear function of the compressive strength. This simplification cannot be applied to any concrete, not even when PC only is concerned. As for the ultimate strength value, due to the long waiting period before complete hydration, its actual measurement is generally not adapted. Determining this parameter by the least square method can give variable results depending on the number of fitting points, and more essentially on the range of α within which the fitting is made. However, it is interesting to note that the RMSE is generally low for any concrete composition. This indicates that this model is adapted to link the strength evolution to the degree of hydration of all tested compositions. Therefore, while its parameters can hardly be predicted, their experimental calibration for a given mix design allows an adequate description of concrete strength through the whole hydration process.

The values of $a_{ft}/a_{fc} < 1$ shown in Table 3 indicate that tensile strength develops faster, and reaches more quickly its final value than compressive strength. This well-known fact is confirmed for all compositions. Its value can vary from one concrete to the other, and the values obtained here are consistent with the range of $0.5 < a_{ft}/a_{fc} < 0.87$ suggested in Ref. [14]. In average, the value of 2/3 used by several authors is confirmed to be an efficient first approximation. However, the ratio between the ultimate tensile

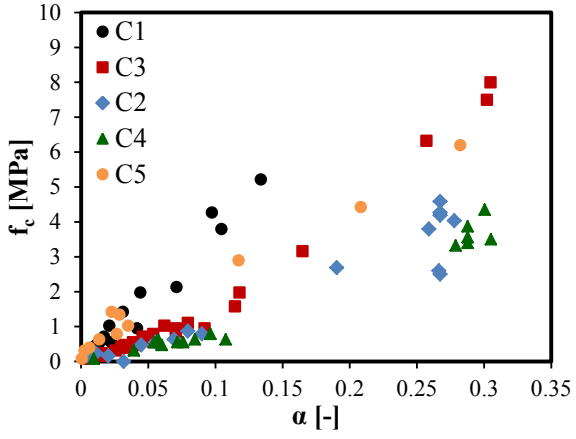

Fig. 3. Very early strength gain as a function of degree of hydration.

Table 3
Ratio of the hydration model parameters of tensile strength to compressive strength.

		C1	C2	C3	C4	C5
$f_{t\infty}/f_{c\infty}$	[–]	0.85	0.88	0.72	0.60	0.76
a_{ft}/a_{fc}	[–]	0.075	0.078	0.076	0.074	0.095

Table 4
Values of the parameters of hydration-based, time-based and UPV-based models and corresponding RMSE for tensile strength and compressive strength.

			Compressive strength					Tensile strength				
			C1	C2	C3	C4	C5	C1	C2	C3	C4	C5
$X = f(\alpha)$	X_∞	[MPa]	62.1	47.5	47.2	44.2	37.4	4.67	3.69	3.59	3.25	3.56
	a_x	[−]	1.2	2.3	2.0	2.4	1.6	1.0	2.0	1.4	1.5	1.3
	RMSE	[MPa]	2.0	1.5	2.9	1.6	2.6	0.12	0.10	0.09	0.11	0.09
$X = f(t_e)$	b_x	[−]	20.0	59.8	29.1	64.0	23.9	17.1	60.5	19.7	43.9	21.6
	RMSE	[MPa]	2.2	1.2	1.9	1.5	0.8	0.14	0.16	0.14	0.10	0.12
$X = f(E_d)$	c_x	[−]	2.71E-05					2.70E-05				
	d_x	[−]	3.687					3.051				
	RMSE	[MPa]	2.4	4.8	1.9	1.7	1.3	0.25	0.68	0.15	0.07	0.27

and compressive strength, also significantly varies. The knowledge of f_c is therefore not sufficient for the estimation of f_t, and the relationship between both is composed of a kinetics parameter and of an amplitude parameter, both of which are dependent on the concrete composition.

3.2.2. Time model

Time-based models are interesting in the way that they do not require the measurement of α, which is often a delicate matter which requires specific experimental tools. Such models are specifically useful for practical reasons, when a specific strength is necessary before removing the formwork on a construction site, or when pre-stressing a concrete beam. However, most of these models contain several parameters, and are not often adapted to specific concrete or even to very early age behaviour [26]. Time-dependent models are really interesting if their mathematical expression is able to estimate f_t or f_c from setting to at least 1 month, depending on as low parameters as possible and on the 28 days strength value, which is generally known. An example of such model is provided in Eq. (10). It is based on one parameter b_x and on the strength at 28d X_{28}. This model has the advantage of being adaptable to any concrete composition, and of being more representative of the early age development than the equation suggested in the Eurocode 2 (EC2 [27,32]), as shown in Fig. 5. Contrary to the hydration model, there is only one fitting parameter, since X_{28} is supposed to be known.

$$X(t_e) = X_{28} \cdot e^{-\frac{b_x}{t_e}} \tag{10}$$

However, this model does not represent accurately the strength evolution after 28 days, contrary to the EC2 model which provides an accurate estimation of strength between 28 days and 1 year.

3.2.3. UPV model

An exponential relationship exists between the compressive strength and P-wave velocity (Eq. (11)), which parameters are clearly affected by several composition parameters (cement type, w/c, and aggregates) [21–23]. Similar exponential relationships have also been observed for the tensile strength evolution [33]. For both properties, it is observed that the nature of the binder influences the V_P-f_c or V_P-f_t relationship. In addition, such a model is theoretically unjustified for the pre-setting and setting behaviour. During the dormant period, strength is negligible while the P-wave velocity yields between 250 and 500 m/s in aired concrete. According to such a modelling strategy, there is a residual strength around 0.4 MPa developed for $V_P = 250$ m/s [24]. According to [34], the same equation can be used for determining the very early strength gain development, but such approach results in parameters m and n in Eq. (11) that are not adapted for the prediction of later age strength.

$$X(V_P) = m \cdot e^{n \cdot V_P} \tag{11}$$

$$X(E_d) = c_x \cdot E_d^{d_x} \tag{12}$$

On the other hand, the dynamic elastic properties are more sensitive to the hardening process than P-waves only [19], which are especially sensitive to the very early build-up of continuous solid paths. The f_c-E_d relationship shown in Fig. 4 exhibit much less dependency to the binder composition or w/b ratio. The f_t-E_d relationship exhibits similar trend. The well-known power model existing between compressive strength and static elastic modulus can therefore be adapted and used for the prediction of f_c or f_t from E_d [25]. The parameters c_x and d_x in Eq. (12) are listed in Table 4. The advantage of this model is that c_x and d_x are not dependent on the binder composition or w/c ratio, and that they are applicable both to the very early age strength gain and to the hardening process. However, these values were only verified up to 7 days. Longer term measurements should be performed in order to verify the validity of this model to hardened specimens.

3.2.4. Strength modelling

The three models of Eqs. (9), (10) and (12) as well as the EC2 prediction are confronted with experimental data for f_c and f_t in Fig. 5 for compositions C1 and C4. During the first week, the most efficient prediction strategy is to deduct strength from the dynamic elastic modulus obtained through the ultrasonic method, since it is dependent on fewer material properties as the other models, which must be calibrated for any tested composition. On the other hand, the time model is also very effective for the prediction of the hardening behaviour of concrete up to 28 days, and presents the

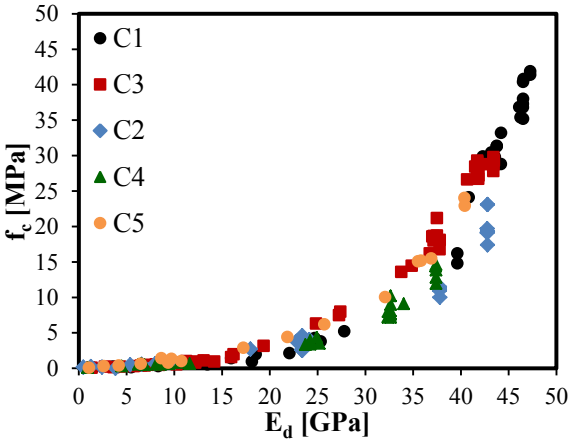

Fig. 4. Compressive strength development as a function of E_d for all compositions.

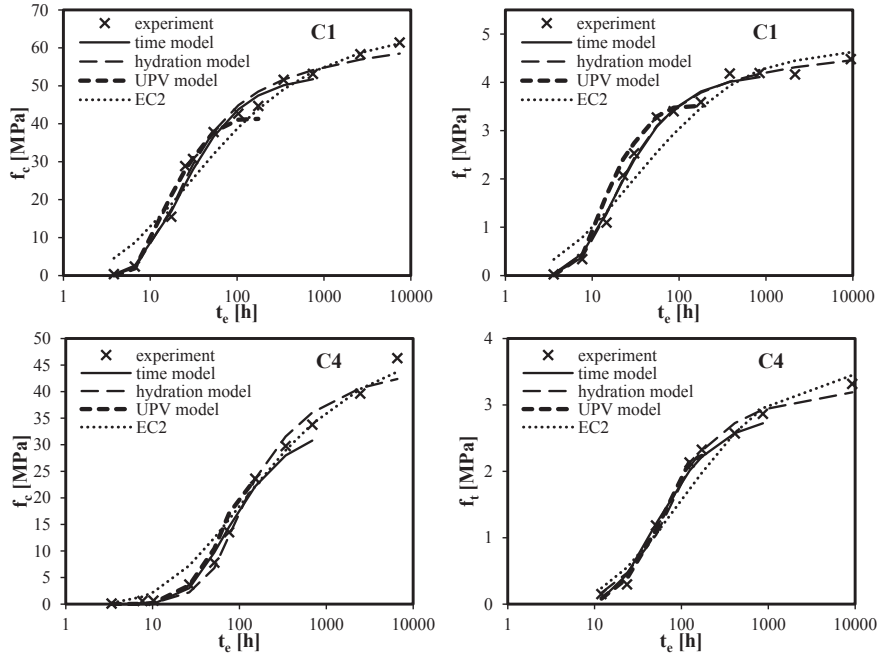

Fig. 5. Comparison between various modelling tools for the evolution of compressive and tensile strength of concrete.

advantage of needing the calibration of only one parameter, provided that $f_{c,28}$ or $f_{t,28}$ are known. Alternatively, the hydration model accurately represents the whole strength evolution, from the setting time up to 1 year. It is also confirmed that the EC2 model is mostly efficient for the extrapolation of concrete strength after 28d up to at least 1 year. This is especially true for the compressive strength, whereas for tensile strength, the hydration model shows a better agreement.

3.3. Elastic modulus

Two experimental methods were used for the measurement of elastic modulus: an extensometer, resulting in individual, punctual values, and a TSTM device, resulting in a semi-continuous measurement through a cyclic methodology. In each case, the static tangent elastic modulus E_s was computed by linear regression between the stress and strain evolution between 20% and 90% of the applied load. Both methods show a good agreement, as already reported in Ref. [26]. This observation is confirmed for the five tested concretes in Fig. 6. Each data point obtained from the extensometer results from the average of three samples issued from two different batches.

As for the tensile strength, C5 and C3 show similar trends. C3 exhibits a slightly higher stiffness for a lower clinker content, which demonstrates once more the interesting contribution of limestone filler. C2 and C4 also present very similar evolutions. As for the compressive and tensile strength, C4 has a faster initial increase up to 1d. Then, the delayed hydration of slag induces a decrease of E_s in comparison with C2. However, in contrast with strength, the presence of slag does not impact the long term properties, even considering that part of it might not be reactive. In fact, the long term E_s in presence of slag is expected to be higher than without slag. This can be explained by the fact that contrary to strength, stiffness can be computed by analytical models which consist in averaging the individual properties of the heterogeneous materials in the sample depending on their respective volume. This means that an inert material does not need to contribute to the hydration reaction, to contribute significantly to the stiffness development. The same three modelling strategies as applied for the strength development are used, based on the degree of hydration, on the equivalent time, and on the dynamic elastic modulus.

3.3.1. Hydration model

In the same way than for the strength modelling, the experimental evidence presented in Fig. 7 shows that there is no identifiable α_0 before which no E_s development has yet occurred. On the contrary, an increase in stiffness can be seen as soon as the hydration reactions start. However, in contrast with the strength evolution, an inversion of curvature can be seen at very early age,

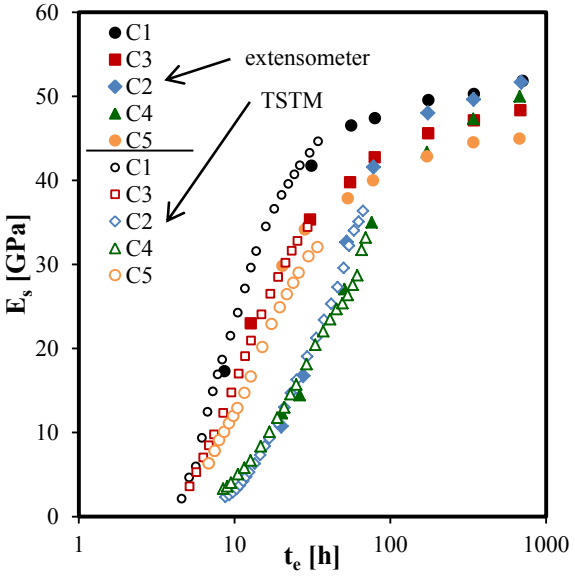

Fig. 6. Evolution of the static elastic modulus obtained from extensometry and TSTM measurements.

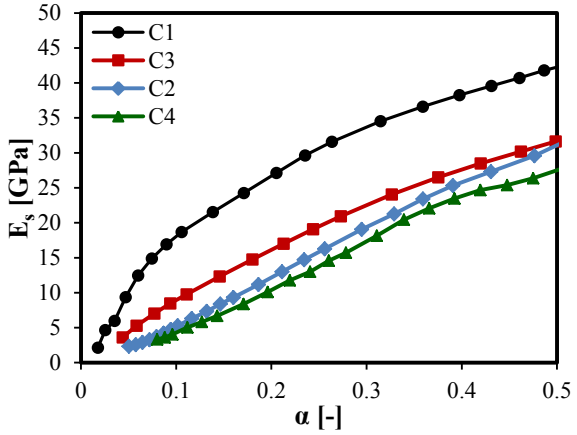

Fig. 7. Very early age stiffness gain as a function of hydration degree.

especially when this initial increase is slow such as in the case of mix designs containing slag. This observation was already made by Krauss and Hariri, who suggested improving Eq. (8) [16]. They observed that there is a linear evolution of E_s between the end of the dormant phase and a given degree of hydration.

Based on this observation and on the obtained results, a new model is proposed, including the observation that the linear trend starts for $\alpha = 0$. The transition between the linear and the power model occurs at $\alpha = \alpha_t$. The parameters α_t and α_0 are obtained by fitting with experimental curves and are not associated to any specific point in hydration or material property. The values of the parameters of the model are shown in Table 5.

$$\begin{cases} E(\alpha < \alpha_t) = E_\infty \cdot \left[\frac{\alpha(t)}{\alpha_t} \cdot \left(\frac{\alpha_t - \alpha_0}{1 - \alpha_0} \right)^{a_x} \right] \\ E(\alpha \geq \alpha_t) = E_\infty \left(\frac{\alpha(t) - \alpha_0}{1 - \alpha_0} \right)^{a_x} \end{cases} \quad (13)$$

It is observed that the transition between a linear and a power increase occurs close to a degree of hydration of 0.1 in the absence of BFS and 0.2 when it is present. In parallel, the values of α_0 are lower than described in Ref. [14] and ref [16]. This is attributed to the lack of very early age measurement of E_s in these experimental studies, where the earliest measurements were performed at a relative development of E_s of around 20%. The specific TSTM device used in this study allows measurements before E_s has reached 5%–10% of its ultimate value.

Table 5
Values of the parameters of hydration-based, time-based and UPV-based models and corresponding RMSE for the static elastic modulus.

			C1	C2	C3	C4	C5
$X = f(\alpha)$	α_t	[−]	0.09	0.20	0.14	0.18	0.11
	α_0	[−]	0.06	0.13	0.06	0.10	0.05
	E_∞	[MPa]	54.2	55.6	47.9	53.4	45.9
	a_x	[−]	0.4	0.7	0.5	0.8	0.6
	RMSE	[MPa]	1.1	0.9	0.8	0.8	1.6
$X = f(t_e)$	τ	[−]	1.4	1.2	1.1	0.9	1.2
	b_x	[−]	8.8	28.0	10.9	29.2	12.1
	RMSE	[MPa]	1.4	1.6	0.9	1.5	1.5
$X = f(E_d)$	c_x	[−]			0.15		
	d_x	[−]			1.52		
	RMSE	[MPa]	1.5	1.5	1.9	1.3	2.1

3.3.2. Time model

The increase of E occurs much faster than compressive or tensile strength. By the time compressive strength reaches 10% of its ultimate value, the elastic modulus has already increased up at least 40% of its ultimate value. The time-dependent models described previously for strength are therefore not applicable to the elastic modulus. This accelerated kinetics can be easily taken into consideration by adding an exponent τ in Eq. (10), resulting in Eq. (14).

$$E(t) = E_{28} \cdot e^{-\left(\frac{b_x}{t}\right)^{\tau}} \quad (14)$$

Fig. 9 indicates that this time model is particularly accurate for representing the early age behaviour in comparison with the EC2 model, which tends to provide widely overestimated E_s values during that time range.

3.3.3. UPV model

Dynamic measurements such as the ultrasonic method imply very low loading amplitude with a high strain rate. Due to the non-linear effect of these factors on the stress-strain relationship [26,29,35], dynamic measurements generally result in higher Young's modulus. A linear relationship is generally accepted between both measurements. However, there is no clear trend regarding the experimental values obtained for the parameters of this linear trend [29,36,37]. In addition, very few results are available for very early age concrete (before 1 day), and there is a clear lack of early age results on different concrete compositions, allowing to assess the effect of cement composition, water/cement ratio or aggregate content. Therefore, the linear relation can hardly be expected to provide good results when E_s is close to 0. It is probable that the static and dynamic measurements of E are more divergent at very early age due to the high viscoelastic properties.

From a theoretical perspective, as soon as E_d increases, there is a corresponding increase of E_s. In other words, if either one of E_s or E_d is null, so is the other. A more accurate relationship between both properties should therefore include this condition. This is confirmed in the present study, as experimental points obtained at very early age effectively deviate significantly from this linear trend. It can in fact be observed that the E_s increases can be modelled as a power law function of E_d (Eq. (15)). Such non-linear relationship was already observed by Refs. [38], who suggested a more complex two-parameter exponential relationship (Eq. (16)).

$$E_s = c_x E_d^{d_x} \quad (15)$$

$$E_s = E_d(1 - ke^{-l\,E_d}) \quad (16)$$

While Eq. (15) mathematically traduces the observation that initially, $E_d = E_s = 0$, it eventually leads to $E_s > E_d$ which is theoretically impossible. The condition $E_s \leq E_d$ is satisfied in Eq. (16) which ensures that E_s tends towards E_d. This is generally verified for materials with low viscous behaviour, such as steel [39] or hardened concrete with no residual free water [40]. In any case, both models successfully represent the early age and hardening relationship between E_d and E_s, as shown in Fig. 8, where the results for all compositions are expressed. Most interestingly, the relationship between dynamic and static measurements is mostly independent on the nature of the binder (SCM content and nature or w/c ratio). This was already observed for the development of compressive and tensile strength. It also corroborates the findings of [19], which observed that the relationship between E_d and the penetration resistance up to the setting time was independent on

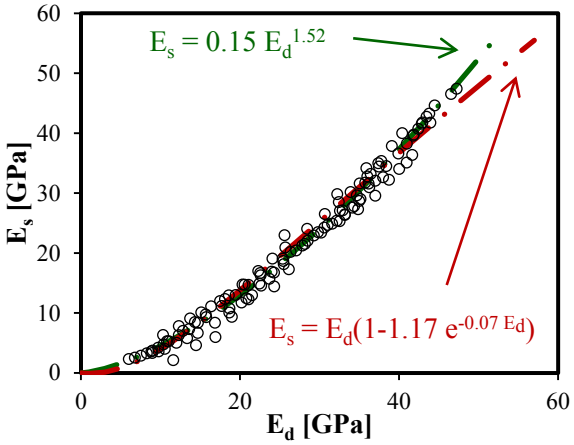

Fig. 8. Relationship between dynamic and static elastic modulus for all tested concrete compositions.

the w/b ratio, amount and nature of fly ash, and air content on mortar samples.

Ultimately, since there is no unambiguous definition of "dynamic" or "static" elastic modulus, the relationship between both measurements is expected to depend on both the loading strain rate and the loading amplitude of their measurement. Additionally, the viscosity of the cement-based material is of upmost importance. The amount and nature of aggregates might therefore affect these relationships, especially at early age. The effects of water content, and nature and amount of aggregates on the relationship between both properties are currently under investigation.

3.3.4. *Elastic modulus modelling*

The three models of Eqs. 13–15 as well as the EC2 prediction are confronted with experimental data for E_s in Fig. 9 for compositions C1 and C4. Except for EC2, all models exhibit very good prediction of all compositions from very early age to hardened concrete. On the other hand, the EC2 model clearly fails to represent the early age increase of E_s. Alternatively, it is observed that the elastic modulus can be determined from the compressive strength according to the well-known power law relation with parameters as fixed in Eq. (17). This is in agreement with values observed in Refs. [14], and validates this prediction methodology even for very early age measurements.

$$E_s = 9.66 f_c^{0.43} \tag{17}$$

4. Conclusion

From the comparison of destructive measurements and continuous non-destructive measurement of ultrasonic P- and S-wave transmission velocity and heat flow of concrete containing various amounts of limestone filler, blast-furnace slag and water/cement ratio, it is observed that:

- Important conceptual adaptations are made to the classical hydration models of concrete mechanical properties. The measurement of fc, ft and Es from the setting time indicates that after the dormant period, all hydration products result in an increase of these mechanical properties. This is in contradiction with the general consensus according to which, before a given degree of hydration, concrete presents no strength or elastic modulus.
- Various models are tested for the determination of the evolution of the tensile and compressive strength and of the elastic modulus. It is shown that the effect of w/b ratio and the presence of BFS and/or LMF on these properties can be accurately accounted for by time-based, hydration-based and UPV-based models. This indicates that strength and stiffness of concrete with massive substitution of clinker by limestone filler and/or blast-furnace slag can be modelled with the same equations as Portland cement concrete, only the parameters of these models are modified by the presence of these mineral additions.
- Provided that their parameters are accurately determined, these models can be used both for the very early age or hardened concrete behaviour. The UPV-based and time-based models are especially best suited for the early age behaviour, while the hydration-based models can be more accurately used for longer term predictions.
- The model of concrete tensile and compressive strength as specified in Eurocode 2 fails to provide accurate prediction for the early age period. In the same way, the Eurocode 2 model widely overestimates the elastic modulus of concrete at early age and during the hardening phase.
- For the early age determination of concrete strength or elastic modulus, the ultrasonic method is the most well suited method. Indeed, it is a continuous non-destructive method, which is directly applicable at the concrete scale, contrary to isothermal calorimetry. In addition, in-situ measurements can easily be performed, which is of valuable interest in many practical applications.
- The UPV-based prediction of strength and stiffness presents the advantage of being independent on the nature of the binder and on the w/b ratio. Therefore, it is expected that the calibration of the model parameters is not necessary if slight variations in the

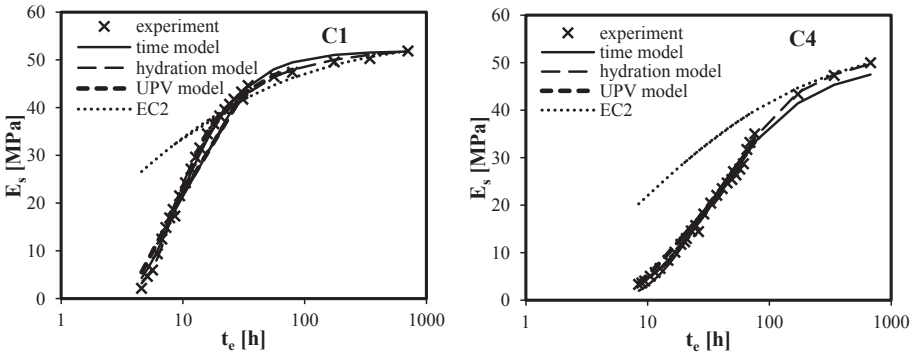

Fig. 9. Comparison between various modelling tools for the evolution of the static elastic modulus of concrete.

nature of the binder is made. A two parameter power law can be used in order to determine f_c, f_t and E_s from E_d.

Acknowledgments

The authors would like to thank the Belgian Fund for scientific research (FNRS) and the Fund David & Alice Van Buuren for their financial support.

References

[1] J. Carette, S. Staquet, Monitoring and Modelling the Early Age and Hardening Behaviour of Eco-concrete through Continuous Non-destructive Measurements: Part I. Hydration and Apparent Activation Energy, Cement and Concrete, Composites, http://dx.doi.org/10.1016/j.cemconcomp.2016.07.002
[2] Report of ACI Committee 233, Slag Cement in Concrete and Mortar, ACI 233R-03, American Concrete Institute, Farmington Hills, Mich, 2003.
[3] P.D. Tennis, M.D.A. Thomas, W.J. Weiss, State-of-the-Art Report on Use of Limestone in Cements at Levels of up to 15%, SN3148, Portland Cement Association, Skokie, Illinois, USA, 2011, p. 78.
[4] G. Menéndez, V. Bonavetti, E. Irassar, Strength development of ternary blended cement with limestone filler and blast-furnace slag, Cem. Concr. Compos. 25 (2003) 61–67.
[5] M.S. Morsy, M. Heikal, Effect of curing temperature on the termal expansion and phase composition of hydrated limestone-slag cement, Ceramics-Silikáty 43 (2004) 110–116.
[6] M. Carrasco, G. Menéndez, V. Bonavetti, E. Irassar, Strength optimization of "tailor-made cement" with limestone filler and blast furnace slag, Cem. Concr. Res. 35 (2005) 1324–1331.
[7] P. Mounanga, M. Bouasker, A. Pertue, A. Perronnet, A. Khelidj, Early-age Autogenous Cracking of Cementitious Matrices: Physico-chemical Analysis and Micro/macro Investigations, Materials and Structures, vol. 44, Springer, Netherlands, 2011, pp. 749–772.
[8] Y. Gao, G.D. Schutter, G. Ye, Z. Yu, Z. Tan, K. Wu, A microscopic study on ternary blended cement based composites, Constr. Build. Mater. 46 (2013) 28–38.
[9] M. Bouasker, N.E.H. Khalifa, P. Mounanga, N.B. Kahla, Early-age deformation and autogenous cracking risk of slag-limestone filler-cement blended binders, Constr. Build. Mater. 55 (2014) 158–167.
[10] L. Courard, F. Michel, Limestone fillers cement based composites: effects of blast furnace slags on fresh and hardened properties, Constr. Build. Mater. 51 (2014) 439–445.
[11] Schindler, Prediction of concrete setting, in: Proceedings of the RILEM International Symposium on Advances in Concrete through Science and Engineering, 2004.
[12] B. Desmet, K.C. Atitung, M.A. Abril Sanchez, J. Vantomme, D. Feys, N. Robeyst, K. Audenaert, G. De Schutter, V. Boel, G. Heirman, Ö. Cizer, L. Vandewalle, D. Van Gemert, Monitoring the early-age hydration of self-compacting concrete using ultrasonic p-wave transmission and isothermal calorimetry, Materials and Structures, vol. 44, Springer, Netherlands, 2011, pp. 1537–1558.
[13] J. Hu, Z. Ge, K. Wang, Influence of cement fineness and water-to-cement ratio on mortar early-age heat of hydration and set times, Constr. Build. Mater. 50 (2014) 657–663.
[14] G. De Schutter, L. Taerwe, Degree of hydration-based description of mechanical properties of early age concrete, Materials and Structures, Kluwer Acad. Publ. 29 (1996) 335–344.
[15] I. Pane, W. Hansen, Concrete hydration and mechanical properties under nonisothermal conditions, ACI Mater. J. 99 (2002) 534–542.
[16] M. Krauss, K. Hariri, Determination of initial degree of hydration for improvement of early-age properties of concrete using ultrasonic wave propagation, Cem. Concr. Compos. 28 (2006) 299–306.
[17] H. Lee, K. Lee, Y. Kim, H. Yim, D. Bae, Ultrasonic in-situ monitoring of setting process of high-performance concrete, Cem. Concr. Res. 34 (2004) 631–640.
[18] N. Robeyst, E. Gruyaert, C.U. Grosse, N.D. Belie, Monitoring the setting of concrete containing blast-furnace slag by measuring the ultrasonic p-wave velocity, Cem. Concr. Res. 38 (2008) 1169–1176.
[19] J. Carette, S. Staquet, Monitoring the setting process of mortars by ultrasonic P-wave and S-wave transmission velocity measurement, Constr. Build. Mater. 94 (2015) 196–208.
[20] J. Carette, S. Staquet, Monitoring the setting process of eco-binders by ultrasonic P-wave and S-wave transmission velocity measurement: mortar vs concrete, Constr. Build. Mater. 110 (2016) 32–41.
[21] J. Keating, D. Hannant, A. Hibbert, Comparison of shear modulus and pulse velocity techniques to measure the build-up of structure in fresh cement pastes used in oil well cementing, Cem. Concr. Res. 19 (1989) 554–566.
[22] S. Popovics, J.L. Rose, J.S. Popovics, The behaviour of ultrasonic pulses in concrete, Cem. Concr. Res. 20 (1990) 259–270.
[23] R. Demirboga, I. Türkmen, M.B. Karakoç, Relationship between ultrasonic velocity and compressive strength for high-volume mineral-admixtured concrete, Cem. Concr. Res. 34 (2004) 2329–2336.
[24] G. Trtnik, F. Kavcic, G. Turk, Prediction of concrete strength using ultrasonic pulse velocity and artificial neural networks, Ultrasonics 49 (2009) 53–60.
[25] A. Boumiz, C. Vernet, F. Tenoudji, Mechanical properties of cement pastes and mortars at early ages: evolution with time and degree of hydration, Adv. Cem. Based Mater. 3 (1996) 94–106.
[26] B. Delsaute, C. Boulay, J. Granja, J. Carette, M. Azenha, C. Dumoulin, G. Karaiskos, A. Deraemaeker, S. Staquet, Testing concrete e-modulus at very early ages through several techniques: an inter-laboratory comparison, Strain (2016), http://dx.doi.org/10.1111/str.12172.
[27] CEB–FIB, Structural Concrete – Textbook on Behaviour, Design and Performance, Updated Knowledge of the CEB/FIB Model Code 1990, vol. 1, 1999.
[28] C. Boulay, A. Colson, Un extensomètre à béton éliminant l'influence des déformations transversales sur la mesure des déformations longitudinales, Matériaux Constr. 14 (1981) 35–38.
[29] I. Shkolnik, Effect of nonlinear response of concrete on its elastic modulus and strength, Cem. Concr. Compos. 27 (2005) 747–757.
[30] S. Staquet, B. Delsaute, A. Darquennes, B. Espion, in: Design of a Revisited Tstm System for Testing Concrete since Setting Time under Free and Restraint Conditions RILEM-jci International Workshop on Crack Control of Mass Concrete and Related Issues Concerning Early-age of Concrete Structures, 2012.
[31] C.G. Hoover, F.-J. Ulm, Experimental chemo-mechanics of early-age fracture properties of cement paste, Cem. Concr. Res. 75 (2015) 42–52.
[32] NF EN 206–1, Béton – Partie 1: Spécification, performances, production et conformité, 2004.
[33] D.-Y. Yoo, J.-J. Park, S.-W. Kim, Y.-S. Yoon, Early age setting, shrinkage and tensile characteristics of ultra high performance fiber reinforced concrete, Constr. Build. Mater. 41 (2013) 427–438.
[34] G. Trtnik, M. Gams, Ultrasonic assessment of initial compressive strength gain of cement based materials, Cem. Concr. Res. 67 (2015) 148–155.
[35] I. Shkolnik, Influence of high strain rates on stress-strain relationship, strength and elastic modulus of concrete, Cem. Concr. Compos. 30 (2008) 1000–1012.
[36] S. Popovics, Verification of relationships between mechanical properties of concrete-like materials, Matériaux Constr. 8 (1975) 183–191.
[37] F. Lydon, R. Balendran, Some observations on elastic properties of plain concrete, Cem. Concr. Res. 16 (1986) 314–324.
[38] S.-H. Han, J.-K. Kim, Effect of temperature and age on the relationship between dynamic and static elastic modulus of concrete, Cem. Concr. Res. 34 (2004) 1219–1227.
[39] H. Ledbetter, Dynamic vs. static Young's moduli: a case study, Mater. Sci. Eng. A 165 (1993) L9–L10.
[40] J. Glucklich, O. Ishai, Creep mechanism in cement mortar, J. Am. Concr. Inst. 59 (1962) 923–948.